CrossMark

**RESEARCH PAPER**

# Nanoliter compound-droplet generation with composition variation

James Black[1] · G. Paul Neitzel[1]

**Abstract** A new method for generation of nanoliter-volume, two-phase (compound) droplets with the ability to vary composition (i.e., encapsulant thickness) is presented. Thermocapillary-driven levitation of water droplets, a capability with potential for the improvement of lab-on-a-chip (LOC) processes, requires encapsulation by a secondary, less-volatile fluid that will also avoid the adverse effects of water-surface contamination on the driving surface motion. Key components of the closed system include the droplet generator actuated by a piezoelectric diaphragm, a pressure-control device, and a specialized nozzle for delivery of the encapsulating liquid. Experimental investigations demonstrate how system pressure variations allow composition changes, and voltage waveform input parameters regulate ejection dynamics, necessary for droplet capturing during the levitation process.

## 1 Introduction

The motivation for this work stems from the desire to apply a method of droplet levitation and transport developed by Nagy and Neitzel (2008) to lab-on-a-chip (LOC) processes. This method utilizes thermocapillary-induced changes in surface stress to drive free-surface motion, dragging surrounding gas into the region where contact between the droplet and substrate would normally occur, continuously replenishing the lubricating layer and preventing contact and, therefore, wetting. The lubricating film generates pressure distributions sufficient to support the weight of the droplet, thereby providing a mechanism for levitation; movement of the heating source leads to flow asymmetry that causes the levitated droplet to track the heating source.

The reason compound droplets are needed to employ this transport mechanism for LOC application is the adverse effect surface contamination has on surface properties coupled with the fact that samples of interest in an LOC used for bio-processing are typically aqueous-based. Water has a high surface tension, making these droplets especially susceptible to surface contamination that leads to inhibition of thermocapillary-driven surface flow. Initially studied by Young et al. (1959) for bubbles, thermocapillary-driven droplet transport in the presence of a surfactant was investigated experimentally for liquid drops by Barton and Subramanian (1989). In those experiments, and in subsequent models developed by Chen and Stebe (1997), it is shown that surfactant accumulation in a cap at the high-tension region of the drop can totally retard surface mobility. For the application motivating the present study, this region must remain uncontaminated to allow the surface motion to replenish the lubricating gas layer, thus sustaining levitation. The use of an immiscible encapsulating liquid with a smaller surface tension will presumably allow for more reliable droplet levitation/translation. Another consideration is the volatility of the encapsulated (sample) liquid, given that the desired technique requires heating of the droplet. By choosing an encapsulating liquid such as low-viscosity silicone oil, which is both minimally volatile in the temperature range needed for levitation and of a low enough surface tension such that surface contamination issues are mitigated, we minimize sample evaporation and expect surface motion vigorous enough to enable levitation.

Lab-on-a-chip processes, given the typical 100-μm cross-sectional length scale of microfluidic channels,

✉ G. Paul Neitzel
  paul.neitzel@gatech.edu

[1] George W. Woodruff School of Mechanical Engineering, Georgia Institute of Technology, Atlanta, GA 30332, USA

employ droplets with nanoliter-scale volumes, three orders of magnitude smaller than those used in the proof-of-concept work by Nagy and Neitzel (2008). The interest in the present work is the development of a technique that will generate single, compound droplets on-demand of specified volume fraction.

Existing compound-droplet generation mechanisms, as well as the method presented in this work, are extensions of well-studied methods to generate single-phase droplets. Basaran (2002) surveys methods whose suitability can be explored for the desired application. Gravitational stretching is the simplest and is employed by Planchette et al. (2010) to create a pendant water droplet on a thin wire. This droplet is encapsulated by oil and allowed to break away from the wire under its own weight, creating a compound droplet. A device created by Che et al. (2012) uses a small capillary tube with two alternating fluids flowing within to generate compound-phase droplets that drip from the nozzle orifice. For the present application, gravitational stretching is an undesirable method as surface deformation of the pendant droplet is necessary to induce separation and this is unfeasible for droplets of nanoliter volume, given their size being much smaller than the capillary length (defined shortly). To date, several methods of generating compound droplets have been developed, but none of them are suitable for this application.

As described by Christopher and Anna (2007), microfluidic devices have been designed to generate droplets in multi-phase systems through the use of co-flowing streams (Umbanhowar et al. 2000), cross-flowing streams (Okushima et al. 2004), or flow-focusing geometries (Utada et al. 2005). A method devised by Terwagne et al. (2010) utilizes impacting streams of droplets of immiscible liquids to generate steady streams of droplets with varying composition. Although a similar apparatus could be developed using air as a tertiary fluid to drive droplet breakup, steady streams of droplets are less desirable to the present work than a system that will provide individual droplets on-demand. Electrospray techniques, when utilized with coaxial liquid jets, can produce compound droplets as shown by Loscertales et al. (2002). Electrical discharge from droplet to substrate of any residual charge from the electrospray process would cause failure of the lubricating film and wetting as discussed by Dell'Aversana and Neitzel (2004), an undesirable effect in the desired application.

To achieve the $O(\mathrm{nl})$ volumes of interest, droplets with diameters of $O(150\ \mu\mathrm{m})$ are required, an order of magnitude smaller than the capillary length, $l_c = \sqrt{\sigma/\rho g}$, a diameter threshold for gravitationally induced surface deformation of droplets. Here, $\sigma$ and $\rho$ are the liquid surface tension and density, respectively, and $g$ is the gravitational acceleration. Compound droplets composed of water and silicone oil created by using the gravitationally induced surface deformation method of Planchette et al. (2010) have diameters in the vicinity of the capillary length and, hence, $O(\mu\mathrm{l})$ volumes. Chen and Basaran (2002) have achieved the requisite nanoliter-volume droplets without reducing nozzle size, but the introduction of a second immiscible liquid and the resulting liquid–liquid interface inhibits the use of this technique for the present purpose.

To produce compound droplets with variable constitution and of the volume desired in drop-on-demand mode, a new generation technique is needed. This technique is described in the following.

## 2 Compound-droplet generator design

The design of the compound-droplet generator is based largely on a simple, single-phase drop-on-demand system devised by Yang et al. (1997) and used in recent work by Terwagne et al. (2013). Their design uses a piezoelectric diaphragm in contact with a liquid-filled chamber to initiate droplet ejection and is consistent with piezoelectric inkjet

**Fig. 1** Experimental setup
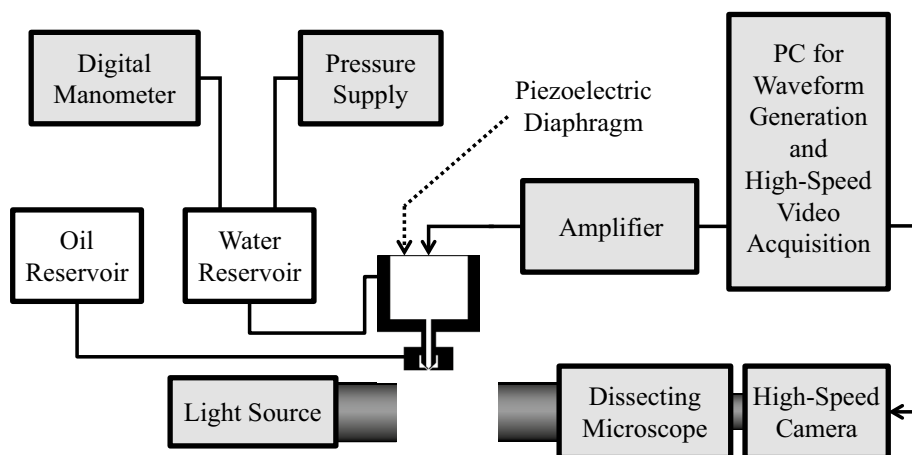
print-head designs (Wijshoff 2010). The present compound-droplet generator, shown schematically in Fig. 1, consists similarly of a diaphragm backing a water chamber driven by a voltage waveform to induce deformation of the membrane and a corresponding pressure pulse leading to droplet ejection. The pressure pulse is dependent on the waveform used and can be modified at will, by changing amplitude, shape, and/or duration to produce the desired droplet ejections.

The ability to generate compound-phase droplets results from the use of a specialized compound nozzle. The compound nozzle is comprised of an inner water nozzle positioned concentrically within an outer oil nozzle, as illustrated in Fig. 2, both of which are machined from stainless steel. The inner orifice is created with a microdrill, and the outer surface is polished to remove defects that could affect droplet ejection. The outer surface of the water nozzle is threaded to permit it to be attached to both the water chamber and the oil nozzle. The water nozzle has an orifice length of 500 μm, diameter of 250 μm, and is coated with a phosphoric-acid-modified perfluoroalkyl chain, which adheres readily to the metallic surface, rendering it hydrophobic to aid in droplet pinch-off. The only surface of the inner nozzle not coated with the hydrophobic coating is the inside of the nozzle orifice to promote the mobility of the liquid–liquid interface necessary for composition variation. The oil nozzle is threaded over the inner nozzle, allowing for differences in axial position between the two, although this feature was not exploited in the results presented here. Its outer surface is coated with a commercial oleophobic coating, Rainoff MFB™, to prevent the silicone oil from wetting this surface and thereby leaking from the oil nozzle.

The water chamber, from which water flows into the inner nozzle, is refilled from a sealed reservoir, allowing for its pressure to be both controlled and varied using a Furness Controls FCO502 Pressure Supply device to a precision of ±1 Pa. This feature is crucial to the repeatable operation of the system and its ability to generate droplets of variable volume ratio.

Oil is gravity-fed into the surrounding outer nozzle; the pressure of the oil is varied by raising or lowering the oil reservoir to change the gravitational pressure head. In a production device, it is anticipated that the oil pressure would be controlled differently to permit more automatic operation on shortened time scales.

## 3 Generation procedure

In order to create a compound droplet, the nozzle must be prepared for ejection. The steps in this process are shown in the illustration in Fig. 2. First, the pressure in the water is set to a value that causes water to partially fill the inner nozzle orifice (Fig. 2a). The oil reservoir is raised to increase oil hydrostatic pressure, causing the oil nozzle to fill with oil (Fig. 2b). The tip of the water nozzle will have space to allow oil to flow into, the size of which is determined by the pressure set within the water chamber. Once the oil overflows the water nozzle, the oil reservoir is lowered to reduce pressure, allowing the excess oil to flow out, thereby leaving an oil-capped water column in the inner nozzle (Fig. 2c). This two-phase column of liquid is what will form the liquid jet to be pinched off into a compound droplet upon actuation. The completion of the process, i.e., the encapsulation of the water droplet by the oil, occurs while the droplet is in free-flight and is driven by the surface properties of the oil/water combination. In the present embodiment, the 5cSt silicone oil quickly [in a time of $O(1 \text{ ms})$; see Fig. 4 below] surrounds the water droplet to form a compound droplet of water encased in oil.



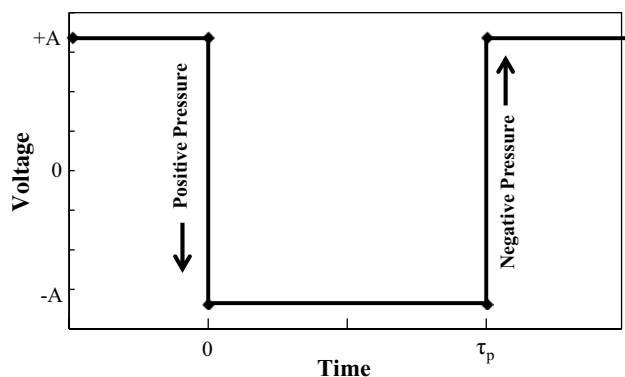**Fig. 2** Nozzle detail and steps in nozzle preparation prior to ejection (**a–c**)
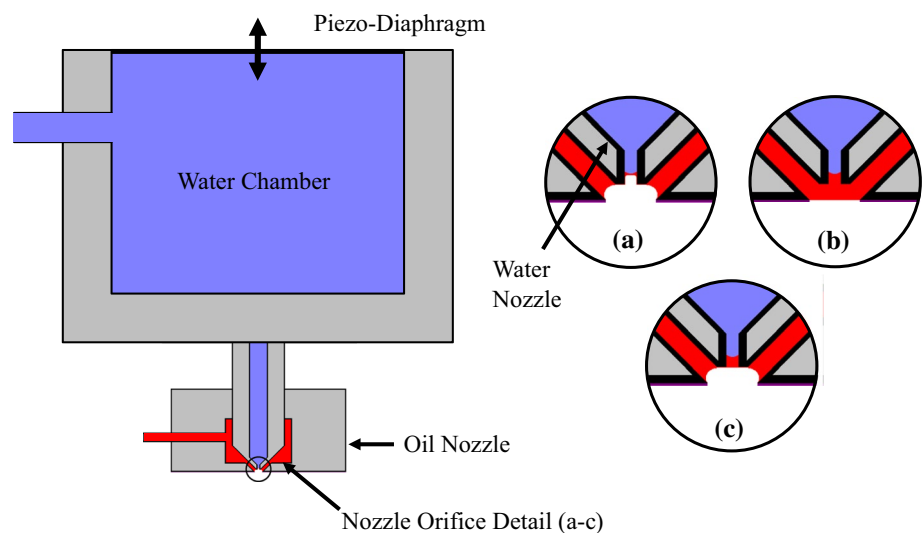
**Fig. 3** Actuating voltage waveform for piezoelectric diaphragm

As mentioned previously, droplet ejection is achieved by providing a pressure pulse via a voltage waveform input to the piezoelectric diaphragm. The waveform used for the results presented in this paper is the square wave shown in Fig. 3. The initial voltage shift (in this case from positive to negative) provides the positive pressure that ejects the liquid contained within the inner nozzle to form a compound tongue of liquid. After a small amount of time, the voltage rapidly shifts again providing the negative pressure that completes the pulse and pinches off the liquid tongue from the nozzle, allowing the formation of the compound droplet. The pulse duration $\tau_p$ controlling the duration of the diaphragm deformation is a key variable in the waveform. Longer pulse durations create a longer liquid tongue, resulting in satellite droplets or multiple droplets. A small range of pulse durations has been found to reliably generate single compound droplets. Within this range, droplet ejection speeds are also dependent on the pulse duration, with the highest (lowest) speeds observed at the largest (smallest) value of $\tau_p$ employed. Modifying the properties of the encapsulated liquid (e.g., increasing viscosity) may be accommodated by changing the pressure-pulse duration, as discussed later. The voltage waveform can also be modified to produce single compound droplets for variable nozzle geometries and operating pressures. Increasing the

amplitude will force liquid out more quickly during the positive pressure portion. Trial and error has been the best method for determining the waveform parameters required to yield a single compound droplet for a given nozzle geometry and chamber pressure.

Representative images of the different stages of droplet ejection are shown in Fig. 4; this case is for a relatively thick encapsulating layer to illustrate the oil–water interface clearly. For these droplets, the amplitude of the waveform output from the amplifier is 67 V and the pulse duration is 185 µs. The times shown in these images are measured from the initial movement of the liquid within the inner nozzle. At $t = 0$, the fluid is actuated, and at $t = 1.25$ ms, the compound liquid tongue is pinched off; the oil plug positioned at the front of the water column is clearly visible. At $t = 1.72$ ms, the pinched-off liquid column with a visible oil–water interface is shown. Deformation as a result of pinch-off oscillation and oil engulfment of the inner droplet is shown at $t = 2.34$ ms. The final image at $t = 3.91$ ms shows a fully encapsulated, virtually spherical, water droplet with the oil–water interface still visible.

Variations in droplet composition are achieved through changes in the water chamber pressure for a fixed pressure pulse, although variation of the latter may also be used, if desired. All water pressures provided are those at the nozzle orifice, with the pressure regulator adjusted to compensate for hydrostatic pressure differences between the free surface in the water reservoir and the location of the nozzle exit. As this pressure is decreased, the water retreats, permitting more oil to flow into the nozzle, leading to a corresponding increase in the amount of oil ejected. This feature allows one to vary the resulting composition of the compound droplet.

## 4 Measurement of droplet composition

Direct measurement of droplet composition cannot be achieved from the high-speed video alone due to the loss
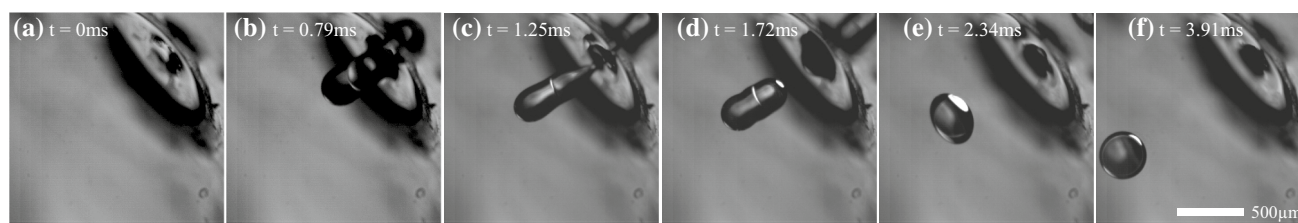


**Fig. 4** Images of compound-droplet formation extracted from high-speed video: **a** Compound nozzle after preparation for ejection; **b** oil–water plug as it begins to exit the nozzle; **c** oil–water plug during pinch-off; **d** oil–water plug immediately following pinch-off; **e** compound droplet as it begins to assume a spherical shape during first oscillation; **f** spherical compound droplet after pinch-off oscillations have fully damped

of information and visibility of the liquid–liquid interface within the compound droplet caused by curvature-induced lensing effects. Additionally, despite the visibility of the oil–water interface in some cases (e.g., in the final image of Fig. 4), the inner-droplet volume cannot be determined from the video images due to the uncertainty of its exact position within the compound droplet. To measure both the compound-droplet volume and the inner water-droplet volume, a more direct approach was taken for which two separate images are analysed. Overall compound-droplet volumes are measured from the high-speed video using a droplet image assumed to be spherical. Therefore, care must be exercised to use an image taken after oscillations induced by droplet pinch-off have damped out. Droplets with an appreciable film thickness (e.g., the droplet shown in Fig. 4) take on a spherical shape within a few milliseconds of ejection. An oscillation damping timescale for droplets composed of mostly water may be estimated as $l^2/v$, where droplet diameter $l$ and kinematic viscosity $v$ are of magnitude $10^{-4}$ m and $10^{-6}$ m$^2$/s, respectively, yielding a 10-ms damping timescale. Droplets containing larger amounts of the more viscous oil will have shorter damping timescales. Higher-resolution videos, in which droplet trajectories are visible longer than 10 ms, are captured and examined to ensure a spherical shape has been reached. Weber number values ($\rho V^2 l/\sigma$) for these droplets are on the order of $10^{-2}$, implying small inertial deformation, thereby validating the spherical assumption of a translating, oscillation-free droplet.

Volumes of the internal water droplet are determined by depositing the compound droplets onto the surface of a bath of 350 cSt silicone oil. The lower viscosity oil film is miscible with the bath liquid, while the highly viscous bath liquid permits a slow descent, with a spherical shape, of the more dense encapsulated water droplet. This allows the suspended water droplet to be photographed through a planar sidewall to avoid optical distortion and its volume determined.

## 5 Results

### 5.1 Effect of water pressure

In order to quantify the droplet composition, we use the dimensionless film thickness, $t_c$, taken to be the thickness of the oil layer divided by the compound-droplet radius, and water volume fraction $F_w$, the aqueous droplet volume divided by the total compound-droplet volume defined as follows:
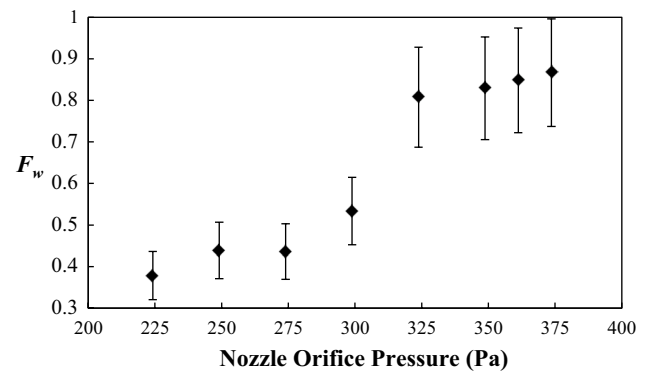
$$t_c = \frac{r_c - r_w}{r_c} \tag{1}$$

**Fig. 5** Water fraction as a function of pressure at the nozzle orifice. The average compound-droplet volume is 23.4 nl
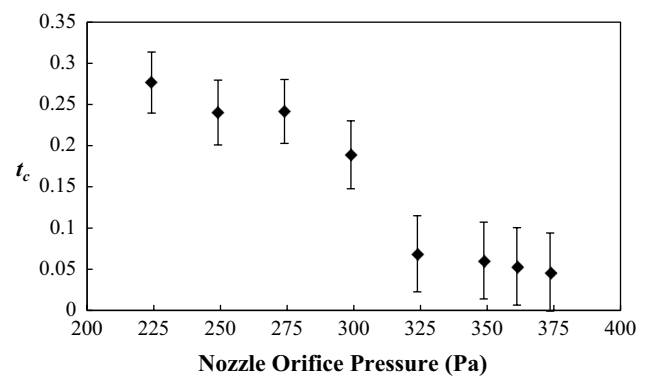
**Fig. 6** Scaled film thickness as a function of pressure at the nozzle orifice. The average compound-droplet radius is 170 μm

$$F_w = \frac{V_w}{V_w} = \left(\frac{r_w}{r_c}\right)^3 = (1 - t_c)^3 \tag{2}$$

In the above, $r_c$ is the compound-droplet radius and $r_w$ the water-droplet radius. Using these quantities, one can determine the composition of the droplet as a function of operating pressure. These results, for fixed pulse duration of 185 μs, are shown in Figs. 5 and 6. Data points in these figures represent averages over multiple droplet ejections, and error bars quantify a computed uncertainty estimate based on image and measurement resolutions using the method of Kline and McClintock (1953). It is clear that, as the pressure at the nozzle orifice is increased, $F_w$ increases while $t_c$ decreases. These trends in water fraction and film thickness are expected since the quantity of oil available for encapsulation is dependent on the location of the oil–water interface within the inner nozzle, which moves as the pressure within the water chamber changes. High water pressures correspond to a location of the water–oil interface at or near the outer surface of the inner nozzle, while lower
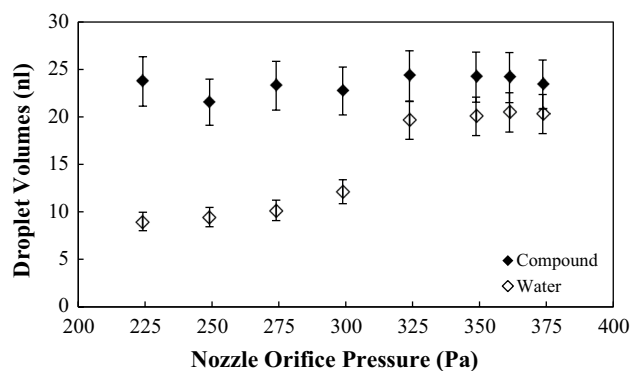
**Fig. 7** Droplet volumes as a function of water chamber pressure

pressures locate the interface farther from the outer surface. Higher pressures than those reported will result in additional increases in the water fraction, including single-phase water droplets, but also yield undesirable effects such as the formation of satellite droplets and forced leaking from the inner nozzle. Lower pressures suppress water-droplet ejection, yielding single-phase oil droplets. An additional effect of decreased oil-layer thickness is manifested through the longer duration of any pinch-off-induced oscillations due to the reduced viscous damping.

The compound-droplet and water-droplet volumes are compared in Fig. 7 below. From this plot, the source of the composition variations can be seen. The inner water-droplet volume increases monotonically with water pressure, as expected. Compound-droplet total volume changes minimally throughout the range of pressures tested, averaging 23.4 nl, which is roughly the same volume as the cylindrical volume (24.5 nl) of the inner nozzle orifice. Assuming that an unchanging waveform yields a minimally varying volume of liquid ejected with variations in composition due solely to the position of the liquid–liquid interface within the inner nozzle, this makes sense. At the upper limit of operating pressures, one expects the water to fill the channel, leading to a "compound" droplet the size of the water droplet alone. As the operating pressure approaches a minimum, the water is nearly sucked back into the nozzle during the negative pressure. Slight necking in the ejected fluid column in the vicinity of the liquid–liquid interface is observed in this case and represents the lower pressure limit of compound-droplet formation.

The trends observed in droplet composition with pressure are a function of the location, shape, and properties of the liquid–liquid interface and metallic surface within the inner nozzle, but not ejection dynamics, as overall compound-droplet volumes remain roughly the same for the pressure pulse used in these experiments. Contributions to composition variations from interfacial shape (i.e., curvature) changes can be estimated directly by relating

the operating pressure to the curvature of the liquid–liquid interface. Reductions (increases) in water (oil) volume as a result of curvature changes alone are an order of magnitude less than the variations observed, and so curvature is assumed to contribute minimally. This suggests that the axial location of the liquid–liquid interface is the driving variable and this is fixed by the operating pressure. A speculation is required regarding the sharp variation in results noted in the neighbourhood of 300–325 Pa of water pressure in Figs. 5, 6, 7. Minor surface irregularities within the inner nozzle orifice could be causing pinning of this interface at one location or another, thereby giving rise to this jump, but internal observation of such features is not possible due to a lack of optical access.

## 5.2 Effect of property variation

In order to more fully characterize the droplet generator operation using different liquids, the inner-liquid viscosity and interfacial tension between the encapsulant and inner droplet are varied by employing mixtures of water and glycerine for the inner liquid. These mixtures are characterized by the weight percent of glycerine. Viscosities are measured using a Canon–Fenske viscometer and interfacial tensions between the mixture and silicone oil are determined using a pendant drop method described by Andreas et al. (1938). The pendant droplets of water-glycerine mixtures are submerged in a 5 cSt silicone oil bath and imaged through a flat glass side panel to obtain surface-curvature images to be used in calculating the interfacial tension. An example of such an image is shown in Fig. 8. Measured values for both kinematic viscosity of the mixtures and the interfacial tension between these and 5 cSt Silicone oil are given in Table 1.

Modifying the inner-liquid properties significantly changes the composition limits of compound droplets produced using the droplet generator developed here. There are two main changes to system parameters that arise from altering the inner-fluid properties. First, a waveform modification must be made to counter the increased inner-liquid viscosity. During droplet ejection, viscous forces have a significant retarding effect on the formation of the jet at the orifice; it therefore becomes necessary to increase the pressure-pulse duration to counter these increased viscous forces. As mentioned previously, a range of pulse durations may be used to successfully achieve a single droplet ejection. Pulse durations are tested and chosen for the inner liquid (with no oil present) to achieve a droplet ejection speed of 0.5 m/s, roughly that observed for the pure water case to match ejection dynamics. Ejection speed as a function of pulse duration is shown in Fig. 9 for a 30 % glycerine mixture. For this liquid, a pulse duration of 210 μs is used (as compared with 185 μs for pure water). Minor changes
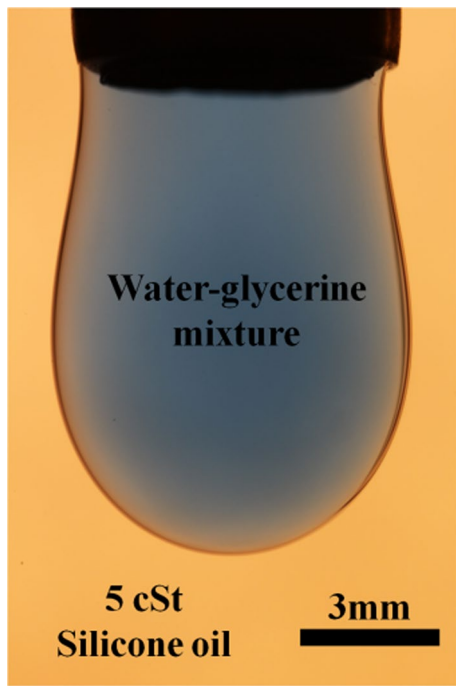
**Fig. 8** Image of a pendant droplet of water-glycerine mixture in a 5cSt silicone oil bath used for measuring interfacial tension

**Table 1** Water-glycerine mixtures and 5cSt silicone oil relevant fluid properties at 22.5 °C

| Glycerine Wt % | $\nu^{a}$ (cSt) | $\sigma^{b}$ (mN/m) |
| --- | --- | --- |
| 0 | 0.95 | 39.0 |
| 10 | 1.33 | 38.1 |
| 20 | 1.66 | 37.3 |
| 30 | 2.20 | 36.7 |
| 40 | 3.38 | 34.9 |
| 50 | 6.10 | 33.2 |

[a] Water-glycerine kinematic viscosity

[b] Interfacial tension between water-glycerine mixture and 5cSt silicone oil

to the pulse duration within the range that produces a single, satellite-free droplet have no effect on the composition of an ejected droplet as composition variation is almost entirely dependent on the location of the liquid–liquid interface within the inner nozzle.

Conversely, the decreased interfacial tension between the water-glycerine mixtures and oil has a significant effect on composition limits. As this tension decreases, the range of operating pressures within the nozzle must be decreased to prevent leaking from the droplet generator. The pressure range for operation with a mixture of 30 % glycerine in water is 0–150 Pa, a significant reduction from the range of 225–375 Pa employed for water as
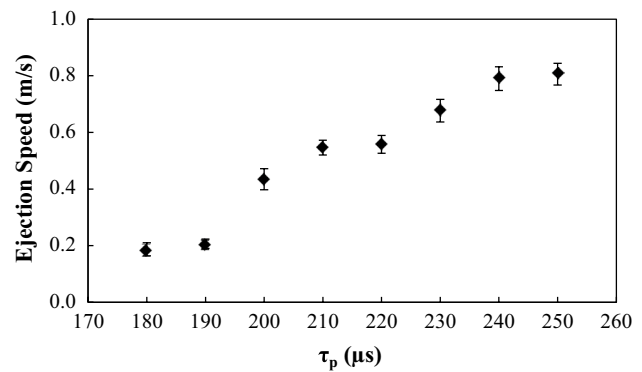


**Fig. 9** Compound-droplet ejection speeds as a function of pressure-pulse duration for 30 % glycerine-water mixtures

the inner liquid. The mobility of the liquid–liquid interface within the inner nozzle is impaired under these conditions allowing only droplets in the upper range of volume fractions (e.g., above 0.8 for the 30 % glycerine mixture) to be produced.

# 6 Conclusions

A technique to generate compound droplets on-demand of varying compositions of silicone oil and distilled water has been developed. Changing the water-reservoir pressure affects the location of the oil–water interface within the water nozzle, causing changes in the volume of silicone oil pushed out of the nozzle ahead of the water. Fluid property variations were also studied to determine how system operation changes with inner liquids of increased viscosity and decreased liquid–liquid interfacial tension. Increases in viscosity are countered easily by lengthening the pressure-pulse duration to match ejection velocities of the pure water case although the interfacial tension reductions drastically restricted the composition range for which compound droplets could be generated. Preliminary experiments suggest that, for LOC applications utilizing infrared laser heating to drive droplet levitation, ejection velocities must be significantly reduced to allow reliable capturing of the compound droplet by the beam. This challenge is overcome by simply changing the pulse duration as described previously to decrease the ejection velocity to a point at which droplet capture is possible.

The technique described here need not be restricted to the LOC application used as its motivation. Other applications calling for encapsulated materials starting in liquid form may also be satisfied using this method.

# References

Andreas JM, Hauser EA, Tucker WB (1938) Boundary tension by pendant drops. J Phys Chem US 42:1001–1019

Barton KD, Subramanian RS (1989) The migration of liquid-drops in a vertical temperature-gradient. J Colloid Interf Sci 133:211–222

Basaran OA (2002) Small-scale free surface flows with breakup: drop formation and emerging applications. AIChE J 48:1842–1848

Che ZZ, Wong TN, Nguyen NT, Chai JC (2012) Formation and breakup of compound pendant drops at the tip of a capillary and its effect on upstream velocity fluctuations. Int J Heat Mass Transf 55:1022–1029

Chen AU, Basaran OA (2002) A new method for significantly reducing drop radius without reducing nozzle radius in drop-on-demand drop production. Phys Fluids 14:L1–L4

Chen JN, Stebe KJ (1997) Surfactant-induced retardation of the thermocapillary migration of a droplet. J Fluid Mech 340:35–59

Christopher GF, Anna SL (2007) Microfluidic methods for generating continuous droplet streams. J Phys D Appl Phys 40:R319–R336

Dell'Aversana P, Neitzel GP (2004) Behavior of noncoalescing and nonwetting drops in stable and marginally stable states. Exp Fluids 36:299–308

Kline SJ, McClintock F (1953) Describing uncertainties in single-sample experiments. Mech Eng 75:3–8

Loscertales IG, Barrero A, Guerrero I, Cortijo R, Marquez M, Ganan-Calvo AM (2002) Micro/nano encapsulation via electrified coaxial liquid jets. Science 295:1695–1698

Nagy PT, Neitzel GP (2008) Optical levitation and transport of micro-droplets: proof of concept. Phys Fluids 20:1–4

Okushima S, Nisisako T, Torii T, Higuchi T (2004) Controlled production of monodisperse double emulsions by two-step droplet breakup in microfluidic devices. Langmuir 20:9905–9908

Planchette C, Lorenceau E, Brenn G (2010) Liquid encapsulation by binary collisions of immiscible liquid drops. Colloid Surf A 365:89–94

Terwagne D, Gilet T, Vandewalle N, Dorbolo S (2010) Double emulsion in a compound droplet. Colloid Surf A 365:178–180

Terwagne D, Ludewig F, Vandewalle N, Dorbolo S (2013) The role of the droplet deformations in the bouncing droplet dynamics. Phys Fluids 25(12):122101

Umbanhowar PB, Prasad V, Weitz DA (2000) Monodisperse emulsion generation via drop break off in a coflowing stream. Langmuir 16:347–351

Utada AS, Lorenceau E, Link DR, Kaplan PD, Stone HA, Weitz DA (2005) Monodisperse double emulsions generated from a micro-capillary device. Science 308:537–541

Wijshoff H (2010) The dynamics of the piezo inkjet printhead operation. Phys Rep 491:77–177

Yang JC, Chien W, King M, Grosshandler WL (1997) A simple piezo-electric droplet generator. Exp Fluids 23:445–447

Young NO, Goldstein JS, Block MJ (1959) The motion of bubbles in a vertical temperature gradient. J Fluid Mech 6:350–356